Tryptophan Fluorescence Quenching by Enzyme Inhibitors As a Tool for Enzyme Active Site Structure Investigation: Epoxide Hydrolase

Evgenia G. Matveeva[a,*] , Christophe Morisseau[b], Marvin H. Goodrow[b], Chris Mullin[c] and Bruce D. Hammock[b]

[a]*Center for Commercialization of Fluorescence Technologies, Department of Molecular Biology and Immunology, University of North Texas, Health Science Center, 3500 Camp Bowie Blvd., Fort Worth, TX 76107, USA;* [b]*Department of Entomology, University of California, Davis, One Shields Ave., Davis, CA 95616, USA;* [c]*Pesticide Research Lab, Department of Entomology, The Pennsylvania State University, PA 16802, University Park, USA*

Abstract: We present the strong fluorescence effect, a new 392 nm emission peak appearing after binding of a naphtol-urea inhibitor XIIa to the enzyme epoxide hydrolase (EH), along with the quenching of the EH tryptophan fluorescence. We have studied the quenching of the 392-nm peak (attributed to XIIa bound inside the active center of the enzyme) of the mixture EH+XIIa by various strong transparent inhibitors (competing with XIIa for binding to EH), and measured the corresponding values of the Stern-Volmer constants, $K(mix)_{SV}$. Strong EH inhibitors demonstrate different replacement behavior which can be used to distinguish them. We further demonstrate a novel fluorescent assay which allows to distinguish highly potent inhibitors and to visualize the strongest among them. We generated our assay calibration curve based on the quenching data, by plotting quenching strength $K(mix)_{SV}$ versus inhibiting strength, IC_{50} values. We used moderate inhibitors for the assay plot generation. We then applied this curve to determine IC_{50} values for several highly potent inhibitors, with IC_{50} values at the limit of the IC_{50} detection sensitivity by colorimetric enzyme assay. IC_{50} values determined from our quenching assay show correlation with IC_{50} values determined in the literature by more sensitive radioactive-based assay and allow differentiating the inhibitors potency in this group. To our knowledge, this is the first inhibitor assay of such kind. Chemical inhibition of EH is an important technology in the treatment of various cardiovascular diseases, therefore, this tool may play a crucial role in discovering new inhibitor structures for therapeutic EH inhibition.

Keywords: Soluble epoxide hydrolase, tryptophan fluorescence quenching, enzyme inhibitors, inhibitor detection.

INTRODUCTION

Epoxide hydrolases (EHs) are enzymes that catalyze the hydrolysis of epoxides or arene oxides to corresponding diols [1, 2]. The role of EHs as detoxifying enzymes has been studied with great interest [2, 3]. An investigation of the inhibition of these xenobiotic-metabolizing enzymes may present an important mechanism in enzyme activity regulation. The EHs are enzymes present in all living organisms; they transform epoxide-containing lipids by adding water. Since many of these lipid substrates carry out important biological functions (such as the regulation of inflammation and blood pressure), the EHs play an important role with profound effects on the physiological state of the host organism [4-6]. There are two major epoxide hydrolases with broad substrate specificity in mammals: the soluble epoxide hydrolase (sEH) and the microsomal epoxide hydrolase (mEH). The mEH is the most active in this regard. A variety of biological data suggests that sEH is involved in the metabolism of endogenous lipids. Thus, the sEH may be a great tool for the development of pharmaceutical agents [5-10], for example, agents that protect against ischemic stroke. The structure of recombinant murine liver EH was reported recently [11, 12].

*Address correspondence to this author at the Center for Commercialization of Fluorescence Technologies, Department of Molecular Biology and Immunology, University of North Texas, Health Science Center, 3500 Camp Bowie Blvd., Fort Worth, TX 76107, USA; Fax: 817-735-2118;
E-mail: ematveev@hsc.unt.edu

Fluorescence detection is an important tool for pharmaceutical detection applications, especially in high-throughput screening assays [13]. Proteins contain three aromatic amino acid residues (tryptophan, tyrosine, phenylalanine) which may contribute to their intrinsic fluorescence. Tryptophan has much stronger fluorescence and higher quantum yield than the other two aromatic amino acids, and tryptophan fluorescence dominates at excitation 280 nm showing a peak with maximum at 330-360 nm. The intensity, quantum yield, and wavelength of maximum fluorescence emission of tryptophan depend on the microenvironment of the tryptophan molecule. The fluorescence spectrum shifts to shorter wavelength and the intensity of the fluorescence increases as the polarity of the solvent surrounding the tryptophan residue decreases. Therefore, tryptophan residues which are buried in the hydrophobic core of proteins, particularly those buried in the enzyme active site, dominate in the fluorescence emission intensity and have spectra shifted by 10 to 20 nm compared to tryptophans on the protein surface.

Fluorescence quenching of the tryptophan residues of proteins by various quenchers (ions, drugs, acrylamide and others) during protein-ligand interaction has been studied in order to confirm the binding site and investigate the mechanism of protein-ligand binding and the nature of the microenvironment of the tryptophan residues [14-19]. From the crystal structure [11, 12] it is clear that there are several tryptophans close to the catalytic site of the enzyme, and we

1389-2010/09 $55.00+.00

have observed changes in fluorescence with the binding of some substrates. Thus, it was hoped that we could develop a rapid assay to evaluate inhibitors of the enzyme binding at the catalytic site by using ligands which altered tryptophan fluorescence.

Substituted ureas and carbamates have been recently reported as potent inhibitors of EH [2, 10, 20-22]. Some of these selective, competitive tight-binding inhibitors with nanomolar K_i values interacted stoichiometrically with the homogenous recombinant murine and human soluble EHs. These inhibitors may become valuable tools for testing hypotheses of involvement of diol and epoxide lipids in chemical mediation *in vitro* or *in vivo* systems.

In this work we investigated the quenching effect of substituted ureas on the tryptophan fluorescence of the soluble EH. Correlation between quenching effects, inhibition power, and structure of inhibitors was discussed. We developed a novel fluorescent assay which allows to distinguish highly potent inhibitors and to vizualize the strongest among them. Tryptophan fluorescence quenching studies of the EH-inhibitor binding can help to understand the toxicological and pharmacological roles of soluble EH.

MATERIALS

Enzyme Preparation

Recombinant mouse sEH was produced in a baculovirus expression system [23, 24] and purified by affinity chromatography [25]. The preparations were at least 97 % pure as judged by sodium dodecyl sulfate-polyacrylamide gel electrophoresis and scanning densitometry. No detectable esterase or glutathione transferase activity, which can interfere with this sEH assay, were observed [26]. Protein concentration was quantified using the Pierce BCA (bicinchoninic acid) assay (Pierce, Rockford, IL). Bovine serum albumin was used as the calibrating standard.

IC_{50} Assay Conditions

IC_{50}s were determined as described using racemic 4-nitrophenyl-*trans*-2,3-epoxy-3-phenylpropyl carbonate as substrate [26]. The enzyme (0.12 μM sEH) was incubated with the inhibitor for 5 min in pH 7.4 sodium phosphate buffer at 30 ^{o}C prior to substrate introduction ([substrate] = 40 μM). Activity was assessed by measuring the appearance of the 4-nitrophenolate anion at 405 nm at 30 ^{o}C during 1 min (Spectramax 200; Molecular Device, Inc., Sunnyvale, CA). Assays were performed in triplicate. By definition, IC_{50} is the concentration of inhibitor, which reduces enzyme activity by 50%. Concentrations of IC_{50} were determined by regression of at least five data points with a minimum of two points in the linear region of the curve on either side of the IC_{50}. The curve was generated from at least three separate runs, each in triplicate, to obtain the standard deviation in Table **1**.

Synthesis of Inhibitors

Compound XXIII was purchased from Aldrich. Synthesis of the compound XIIa is described below. Syntheses of the other compounds are described in the references listed in Table **1**.

1-Cyclohexyl-3-(4-Hydroxy-1-Napthyl)Urea (XIIa)

To a solution of 0.478 g (2.2 mmole) of 90% 4-hydroxynapthylamine hydrochloride and 0.335 g (2.2 mmole) of 1,8-diazabicyclo[5.4.0]undec-7-ene (DBU) in 2 mL of dimethylformamide was added 0.26 mL (0.25 g, 2.0 mmole) of cyclohexylisocyanate over 5 min. After 12 h at ambient temperature, 20 mL of ice-water was added, and the pH lowered from 4 to 2 with 6 M HCl to precipitate a purple-colored solid. Recrystallization of the solid from methanol/water (5:2, v/v) provided analytical material, mp 193 ºC (dec): TLC R_f 0.56 [hexane/ethyl acetate (1:1, v/v)], 0.87 (ethyl acetate); IR (KBr) 3332 (s, br, NH, OH), 1635 (vs, C=O), 1586 (vs, amide II) cm^{-1}; ^{13}C NMR (DMSO-d_6/TMS) δ 155.9 (C=O), 149.6 (ArC-1), 128.8, 126.6, 126.0, 125.0, 124.6, 122.7, 129.1, 120.6, 107.8, 48.0 (C-1), 33.4 (C-2,6), 25.5 (C-4), 24.7 (C-3,5); MS *m/z* (relative intensity) 384 (56, $M + C_6H_{11}NH_2 + H^+$), 285 (100, $M + H^+$), 143 (85, $M + 2H)^{2+}$, 100 (56, $C_6H_{11}NH_2 + H^+$).

METHODS

Melting points were determined with a Thomas-Hoover apparatus (A. H. Thomas Co., Philadelphia, PA) and are uncorrected. Infrared spectra were recorded on a Mattson Galaxy Series FTIR 3000 spectrometer (Madison, WI). ^{13}C-NMR spectra were measured on a General Electric QE-300 spectrometer (Bruker NMR, Billerica, MA) operating at 75.5 MHz. The FAB mass spectra were generated on a Kratos MS-50 mass spectrometer (Kratos Analytical, Manchester, UK) using either glycerol or 3-nitrobenzyl alcohol as the matrix. A Shimadzu UV-2101 PC UV-VIS scanning spectrophotometer was used for absorbance measurements.

Fluorescence measurements in standard 1 cm cuvettes were performed using a Fluoromax II spectrofluorometer, Jobin Yvon – Spex, U.S.A., at room temperature (22 ^{o}C), and excitation/emission slits at 5 nm each. EH fluorescence spectra were taken at excitation 280-290 nm, and emission 334 nm. Quenching of the enzyme (EH) fluorescence in presence of the inhibitors was measured as follows. Two cuvettes were used for measurements, one shortly after the other. The sample cuvette contained 2 ml EH solution in 0.1 M sodium phosphate buffer (pH 7) (immediately after the dilution of the stock EH solution, which was stored on ice) and 2-50 μl of the inhibitor solution in dimethylformamide (DMF). The control cuvette contained same amounts of the EH solution and DMF. Thus, the incubation time (warming of the EH solution in cuvettes) was the same for the sample and control—about 5-30 min. (This consistent incubation time was very important, because after about 60 min, we observed an approximately 30% decrease of EH fluorescence in the control cuvette).

Two-peak Lorentzian fitting for fluorescence spectra was performed using the "Microcal Origin" software, version 4.00, Microcal Software, Inc., U.S.A.

RESULTS AND DISCUSSION

A wide range of different EH inhibitors was tested to determine their effect on tryptophan fluorescence with homogenous recombinant sEH of mice. Tryptophan quenching at low (0.5 mM or less) or high (5 mM) concentration of the

Table 1. Quenching of mEH Fluorescence (at 334 nm) by Various EH Inhibitors

Inhibitor [Ref.][1]	Structure	Mouse sEH IC_{50} (μM)	Quenching, %		K_{SV} (10^6), M^{-1}
			Low I (0.5 mM)*	High I (5 mM)	
I [27]	n-$C_{12}H_{25}$-NH_2	> 500		0 ± 15	
II [28]	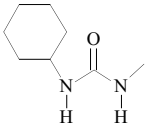	> 500		0 ± 15	
III [27]	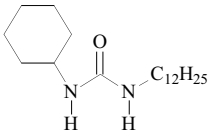	0.05 ± 0.01 0.0098±0.0004 [27]		0 ± 15	
IV [27]	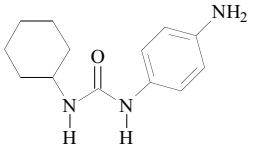	0.17 ± 0.02	10 ± 7 (10 μM)	10 ± 5	0.004
V [29]	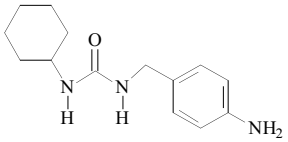	0.05 ± 0.01	5 ± 5 (10 μM)	3 ± 5	0.012
VI [27]	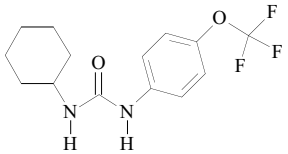	0.05 ± 0.01 0.016±0.0002 [27]	0 ± 10 (10 μM)	-5 ± 10**	-0.001
VII [27]	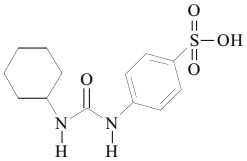	44 ± 1	-4 ± 3		
VIII [29]	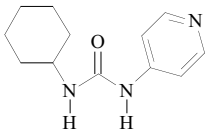	0.07 ± 0.01	-14 ± 5		
IX [27]	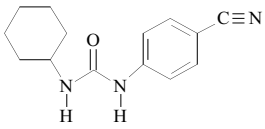	0.06 ± 0.01	-10 ± 5		
X [29]	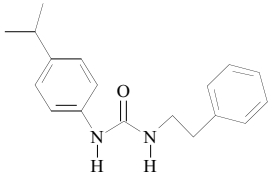	0.20 ± 0.01	0 ± 10 (25 μM)	0 ± 5	0.000

(Table 1) contd....

Inhibitor [Ref.][1]	Structure	Mouse sEH IC_{50} (μM)	Quenching, %		K_{SV} (10^6), M^{-1}
			Low I (0.5 mM)*	High I (5 mM)	
XI [29]	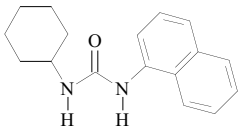	0.85 ± 0.02	-10 ± 5 (5 μM)	-5 ± 20**	-0.044
XIIa [29]	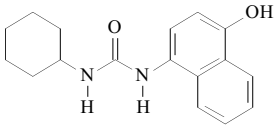	0.65 ± 0.01			
XIIb [29]	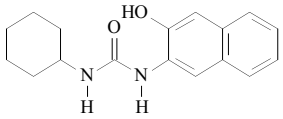	0.05 ± 0.01			
XIIc [29]	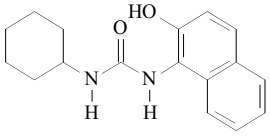	0.05 ± 0.01			
XIII [30]	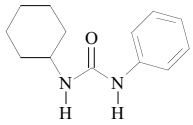	0.284±0.002 [27] 0.76 ± 0.02	0 ± 5	-3 ± 7**	-0.002
XIV [27]	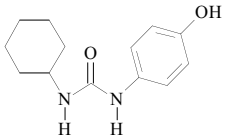	0.8 ± 0.03 [27] 0.79 ± 0.08	6 ± 4		
XV [29]	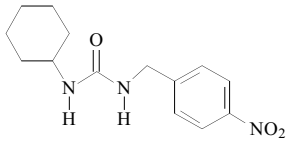	2.3 ± 0.3	40 ± 3 (10 μM)	77 ± 5	0.042
XVI [27]	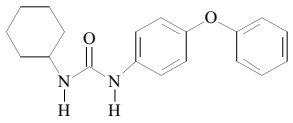	0.05 ± 0.01	35 ± 3 (5 μM)	***	0.107
XVII	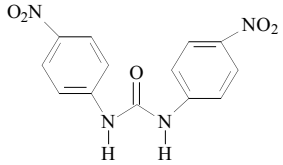	88 ± 11	80 ± 3 (75 μM)	***	0.112
XVIII [27]	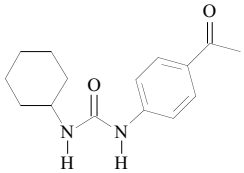	0.06 ± 0.01	100 (75 μM)	100 ± 5	0.164

(Table 1) contd....

Inhibitor [Ref.][1]	Structure	Mouse sEH IC_{50} (μM)	Quenching, %		K_{SV} (10^6), M^{-1}
			Low I (0.5 mM)*	High I (5 mM)	
XIX [30]	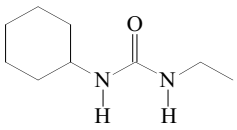	51.7 ± 0.7			
XX [31]	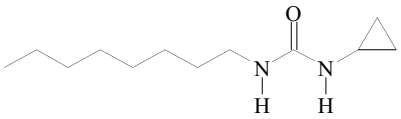	9.51± 0.09			
XXI [27]	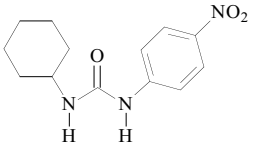	0.17 ± 0.01	65 ± 2 (4 μM)	***	0.471
XXII [29]	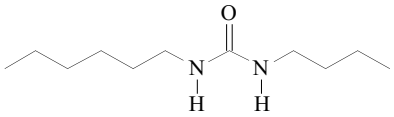	1.7 ± 0.1			
XXIII	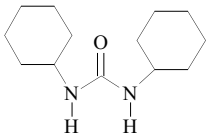	0.0818±0.0007 [27] 0.09 ± 0.01		0 ± 15**	
XXIV [27]	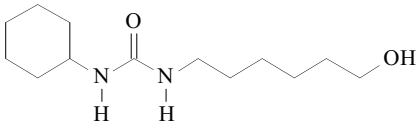	0.181 ± 0.002 [27] 0.05 ± 0.01			
XXV [27]	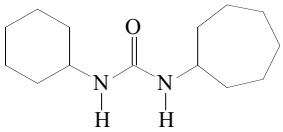	0.0167 ±0.0005 [27] 0.05 ± 0.01			
XXVI [27]	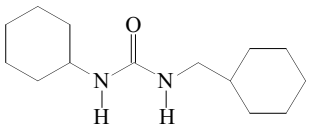	0.0073±0.0001 [27] 0.06 ± 0.01			
XXVII [29]	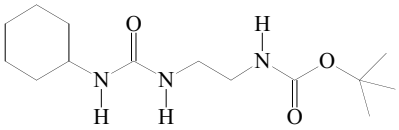	0.05 ± 0.01			

[1]Reference describing the synthesis of the inhibitor. Compound XXIII was purchased from "Aldrich".

* [I] was 0.5 mM or lower; if lower (4 to 75 μM) – the concentration is given in brackets under the quenching value.

** negative quenching means that fluorescence enhancement was present instead of quenching.

*** estimation of quenching not possible due to high fluorescence of the inhibitor itself.

inhibitor, calculated as the ratio of the tryptophan fluorescence (ex 290 nm, em 340 nm) in presence and in absence of an inhibitor, is presented in Table **1**, as well as inhibitor's structures and IC_{50} values. The primary amine which inhibits the microsomal, but not the soluble, EH had no effect on fluorescence (I, Table **1**). All of the sEH inhibitors tested used the urea pharmacophore. In addition, wide range of aliphatic and aromatic substitutents was studied as shown in Table **1**. None of the aliphatic urea derivatives studied significantly altered the emission spectrum of the sEH when excited at 280-290 nm. This suggests that binding of the aliphatic inhibitor to the enzyme does not alter the fluorescent

properties of the tryptophans near the catalytic site. We have studied the quenching effect of a wide variety of aromatic urea derivatives in more detail, at different inhibitor concentrations (see Table **1**). Some of the aromatic urea derivatives were strong quenchers for EH fluorescence while others were not (Table **1**).

Quenching behavior of various aliphatic/aromatic inhibitors varied widely, from no effect (or even slight fluorescence enhancement) to strong quenching up to 100% complete quenching; three representative quenching curves are shown on Fig. (**1**) (slight fluorescence enhancement, no quenching, intermediate quenching, and strong quenching). In order to better quantify the quenching, we calculated the values of the Stern-Volmer constants (K_{SV}) for each inhibitor using Stern-Volmer equation: $Fo/F = 1 + K_{SV}$ [inhibitor], where F and Fo is the fluorescence in the presence and absence of quenching inhibitor, respectively. The values are presented in Table **1** (right column). Stern-Volmer plot was linear only for the initial range of inhibitor concentrations, and showed saturation at higher concentrations, hence, the K_{SV} value was calculated using first 4-6 data points, up to approximately 4-5 μM for strong inhibitors and 25-50 μM for weak inhibitors. Thus, we consider both quenching characteristics (percentage of quenching and K_{SV} values) as semi-quantitative, with percentage related more to higher inhibitor concentrations, and K_{SV} value related more to lower ones.

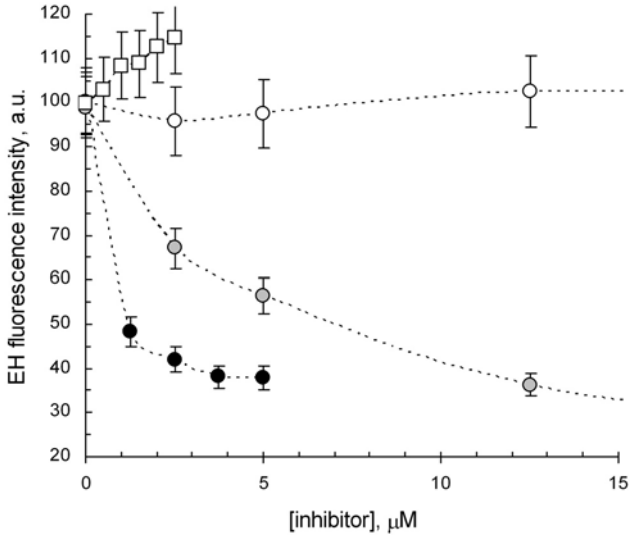

Fig. (1). EH fluorescence (in 100 mM Na-phosphate buffer, pH 7.0), emission 334 nm, in the presence of various aromatic inhibitors: no-quencher VI (white circles, [EH] 25 nM, ex 280 nm); intermediate quencher XVIII (grey circles, [EH] 25 nM, ex 280 nm); and strong quencher XXI ([EH] 125 nM, ex 290 nm). White squares show the effect of slight fluorescence enhancement by inhibitor XI ([EH] 25 nM, ex 280 nm).

After analyzing a wide variety of structures of inhibitors (Table **1**), we found that the strong quenchers were urea pharmacophores, whose structure included a cyclohexyl (or phenyl) residue from one side (R), and phenyl residue from the other side (R'). An electron donor in para-position of the R' (like N^+ in XVII, C^+ in XVIII, S in VII) resulted in quenching, while electron acceptors in the same position of R' were inferior quenchers (O in VI, XIV, and N^- in IV). Phenyl without a para-substitutor (XIII), pyridine (VIII), or aliphatic radicals (I, III) as an R', did not express any quenching effect. A CH_2 spacer between urea's NH and R' leads to the decrease of the quenching effect (compare XV, XVII, and XXI, Table **1**).

The cyclohexyl naphthyl urea (XI, Table **1**) showed a slight tryptophan fluorescence enhancement at increasing inhibitor concentrations (Fig. **1**). Thus, several other naphthyl derivatives were tested (XIIa - XIIc, Table **1**). It was hoped that the resulting compounds might not only alter the tryptophan fluorescence of the sEH itself, but that the fluorescence properties of the resulting naphthol ligands might be altered in the hydrophobic pocket of the enzyme. The effect of the EH on the fluorescence of the naphthyl derivatives XIIa - XIIc (ex 330 nm) is shown in Fig. (**2**). Two of the naphthol derivatives (XIIb, XIIc) showed slight quenching in the presence of sEH (Fig. **2B,C**), however, with the 1,4-naphthol derivative (XIIa) there was an appearance of a new peak and a clear enhancement of fluorescence (Fig. **2A**).

Since compound XIIa yielded the strongest effects of those studied, and resulted in the appearance of a new peak rather than just the disappearance of a tryptophan peak, the interaction of the EH with 1,4-naphthol derivative XIIa was studied in greater detail. Fig. (**3**) shows the fluorescence spectra of various XIIa concentrations in the absence (**3A**) or in the presence (**3B**) of EH. We can see that fluorescence spectra of the inhibitor XIIa inside the active site of EH clearly differ from the spectra of the free inhibitor when excited at 330 nm (at inhibitor excitation maximum), even though EH itself shows no fluorescence when excited at 330 nm.

Next, we studied the fluorescence properties of the XIIa – EH mixtures at the tryptophan excitation (290 nm); the results are presented in Fig. (**4**). We observe here not only the quenching of the EH tryptophan peak at 340 nm, but also the appearance of the new peak at longer wavelengths (approximately 380-390 nm), as the inhibitor concentration increases. This new peak of XIIa, which occurs at the point of interaction with sEH, can clearly be observed in the case of two-peak fitting for the spectrum using Lorentzian fitting (Fig. **5**); this fitting results in the value of 392 nm at the maximum.

In some cases emission the spectrum may be affected by the changes in the local microenvironment of the fluorophore [32]. The peak height then, due to possible maximum shift, is no longer a reliable characteristic of the fluorescence, compared to the area under the spectrum ("peak area"). We tested the behavior of the peak height versus peak area at various concentrations of the inhibitor XIIa and found that both values change uniformly (Fig. **6**). Both the height and the area of the new 392-nm peak show the saturation curve when plotting the height or area against the XIIa concentration (Fig. **6**). From this we can conclude that, at given EH concentration, further increase in the inhibitor concentration after saturation of the enzyme active sites does not result in an increased 392-nm peak fluorescence. This is in agreement with the fact that 290 nm excitation can not result in fluores-

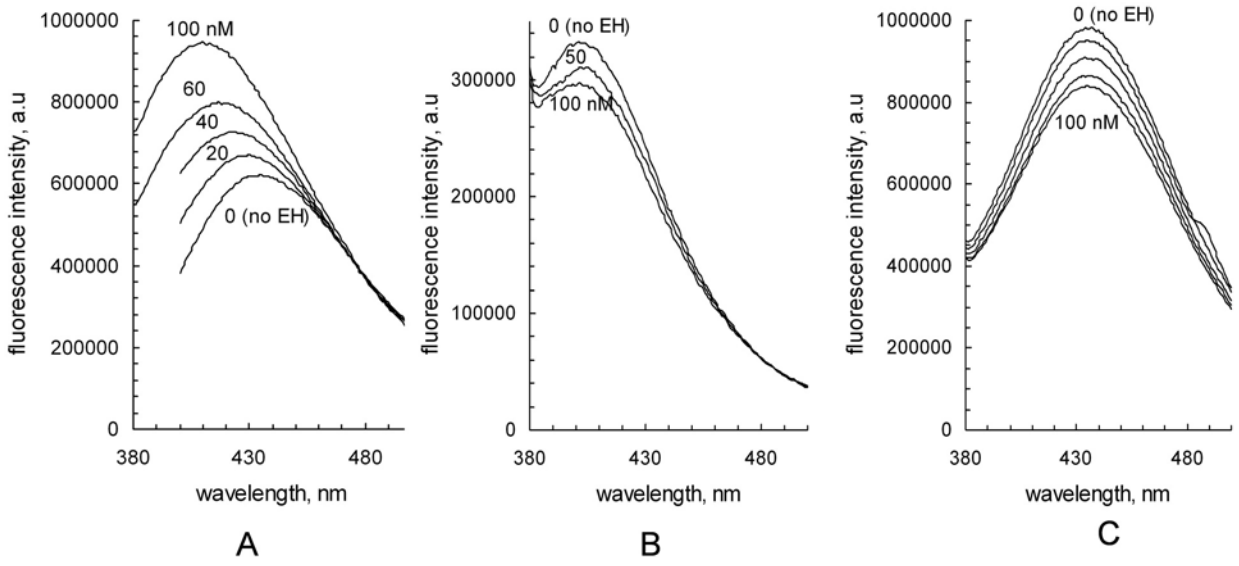

Fig. (2). Fluorescence spectra of XIIa **(A)**, XIIb **(B)**, and XIIc **(C)** (excited at 330 nm) in the presence of varied concentrations of EH (0-100 nM). C: EH = 0, 20, 40, 60, and 100 nM.

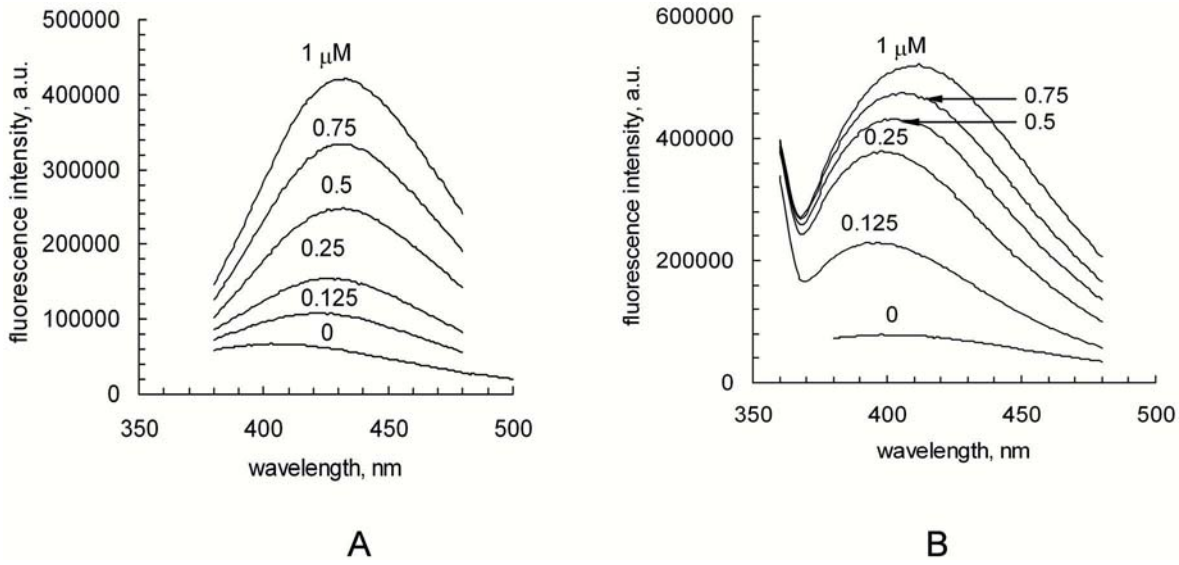

Fig. (3). Fluorescence spectra of XIIa (at excitation 330 nm) in absence **(A)** and in the presence **(B)** of 50 nM EH; [XIIa] varies from 0 to 1 μM.

cence of the free (not bound to EH) inhibitor XIIa (data not shown). Hence, the 392-nm peak can be attributed to the inhibitor bound inside the EH active site; importantly, this peak can be excited by the tryptophan excitation optimum (280-290 nm).

There are two likely mechanisms for this effect. One possibility is that the fluorescence of the 1,4-derivative XIIa becomes blue shifted and strongly enhanced upon binding to the enzyme, because the microenvironment of the fluorophore XIIa is changing from hydrophilic to more hydrophobic. This hypothesis is partially confirmed by the change in the fluorescence spectra of XIIa in buffer versus various organic solvents (Fig. **7**). We see the enhancement of the fluorescence in organic solvents; however, there is no big shift in the excitation maximum due to the solvent effect (Fig. **7**).

An alternate hypothesis is that when the 1,4-naphthol binds to the sEH, it comes within close proximity to one or more excitable tryptophans and, at the tryptophan excitation, there is an energy transfer resulting in the quenching of the tryptophan fluorescence, as well as the "pumping" of the inhibitor's fluorescence by tryptophans and the appearance of the 392-nm peak corresponding to the fluorescence of the XIIa inside the active site. Further investigations, including time-resolved study, are needed to confirm this hypothesis.

The "bound inhibitor" peak arising in the mixture of XIIa and sEH could serve as a tool for inhibiting the potency of the spectrally invisible, 'transparent' EH inhibitors. It is very difficult, and in some cases not possible, to differentiate the best EH inhibitors from each other on the basis of their IC_{50} values [33]. Best inhibitors immediately block active sites of

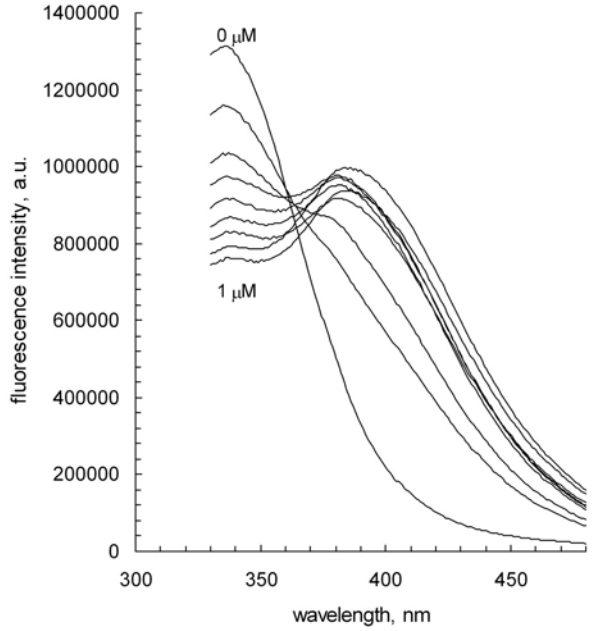

Fig. (4). EH fluorescence spectra (ex 290 nm) in the presence of XIIa: [XIIa] = 0; 0.125; 0.25; 0.375; 0.5; 0.625; 0.75; 0.875; and 1 μM; [EH] = 50 nM.

the EH and do not allow the EH substrate to react. In our case, using a fluorescing molecule such as XIIa, also a very strong EH inhibitor, we can simply monitor the "bound inhibitor" peak while adding some other inhibitors competing with XIIa for the EH active site. When we add 'transparent' inhibitors to the mixture of EH+XIIa, and monitor the 392-nm peak, we see the quenching of this peak by a transparent inhibitor, probably due to the replacement of the XIIa by a 'transparent' inhibitor (if the transparent inhibitor in stronger than XIIa). We have studied the quenching of the 392-nm peak of the mixture EH+XIIa by various strong transparent inhibitors (competing with XIIa for binding to EH). The obtained quenching values (along with inhibitor concentrations) and corresponding values of the Stern-Volmer constants, $K(mix)_{SV}$, are given in Table **2**. Several representative quenching curves are shown on Fig. (**8**). Various strong EH inhibitors demonstrate different replacement behavior – which can be used to distinguish them. An assay for strong EH inhibitors can be generated based on these quenching data, by plotting quenching strength (for example $K(mix)_{SV}$ values) versus inhibiting strength, such as IC_{50} values.

Fig. (**9A**) shows the correlation between IC_{50} of the inhibitors (x) and $K(mix)_{SV}$ values (y). The IC_{50} value of 0.05 μM is the lowest one which can be easily determined by colorimetric enzyme immunoassay (as in this work). This type of assay does not permit the segregation of very potent inhibitors due to its low sensitivity, so inhibitors with these assigned values may have the "real" potency equal to the IC_{50} of lower than 0.05 μM. Hence, we only used the inhibitors with IC_{50} higher than 0.05 μM for our assay calibration curve, namely XIX, XX, XXII, and XXIII, as well as the low-potency inhibitor II with high IC_{50} value and negligible quenching effect (grey circles on Fig. **9A** and Fig. **9B**).

Fig. (**9A**) shows the calibration plot (grey circles) and a set of strong inhibitors with IC_{50} values 0.05-0.06 μM, at the limit of the IC_{50} detection sensitivity by colorimetric enzyme assay (black circles). From Fig. (**9A**) we see that several inhibitors with close IC_{50} values of about 0.05 μM have different quenching potency, which can be an indication of their inhibiting potency: hence, from this group, inhibitor XXVII is the strongest one, inhibitor XXIV is the weakest one, and inhibitors XXV and XXVI are in-between. If we apply our calibration plot to these strong inhibitors and align all the corresponding data points from Fig. (**9A**) along the calibration, as shown by arrows on Fig. (**9A**), we will get a set of data as shown on Fig. (**9B**), white circles, from which we calculated appropriate corrected values of IC_{50} presented in

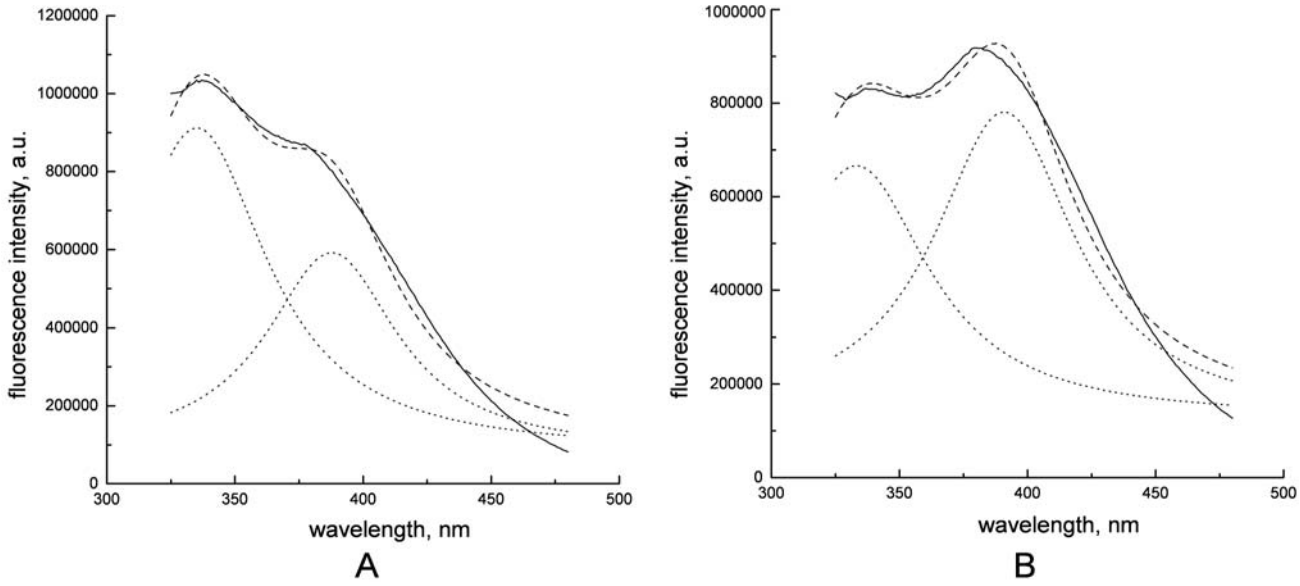

Fig. (5). Lorentzian fitting of the fluorescence spectra of EH + XIIa (excitation 290 nm, [EH] = 50 nM): **A)** [XIIa] = 0.25 μM; **B)** [XIIa] = 0.75 μM. Solid black line – experimental; dashed line – fitting, dotted line – fitting, separate peaks.

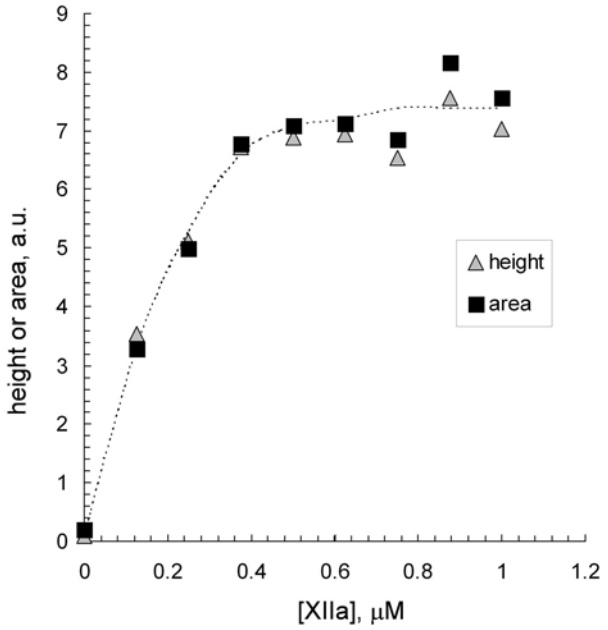

Fig. (6). Height and area (according to the Lorentzian fitting) of the 392-nm fluorescence peak of the mixture EH + XIIa at varied concentrations of XIIa ([EH] = 50 nM).

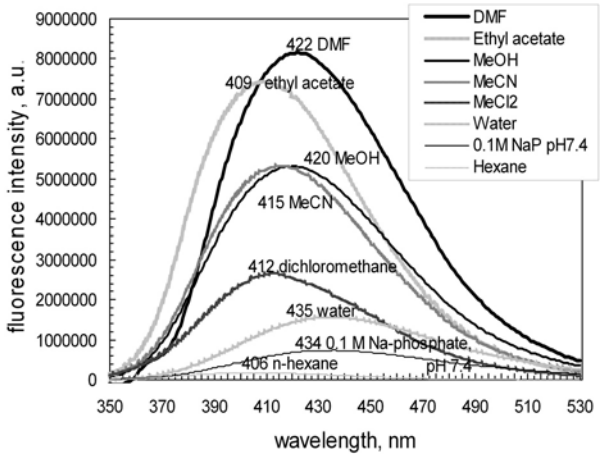

Fig. (7). Solvent effects on fluorescence spectra of XIIa (excitation 300 nm). Numbers in front of the solvent show the emission maximum.

Table **2**, right column. These values show stronger inhibitor potency and allow us to differentiate the potency in this group. They also correspond quite well to the IC_{50} values obtained in the literature [27] by more sensitive radioactive-based assay (Table **2**). Radioactive-based assay allows 10-20-fold improving in sensitivity [27, 34], but this assay utilizes radioactive substrate and involves extraction steps and hence is time- and cost-consuming.

It is notable that two of the best 'non-visible' inhibitors, XXV and XXVI, characterized by the $K(mix)_{SV}$ value more than 1 (Table **2**), have a structure very similar to the structure of the inhibitor XXIII (DCU), with much less inhibitor potency Table **1**). The only difference in the structures is a cycloheptyl R in XXV or a cyclohexyl with a single CH_2 spacer in XXIV, compared to a cyclohexyl R in XXIII (see Table **1**).

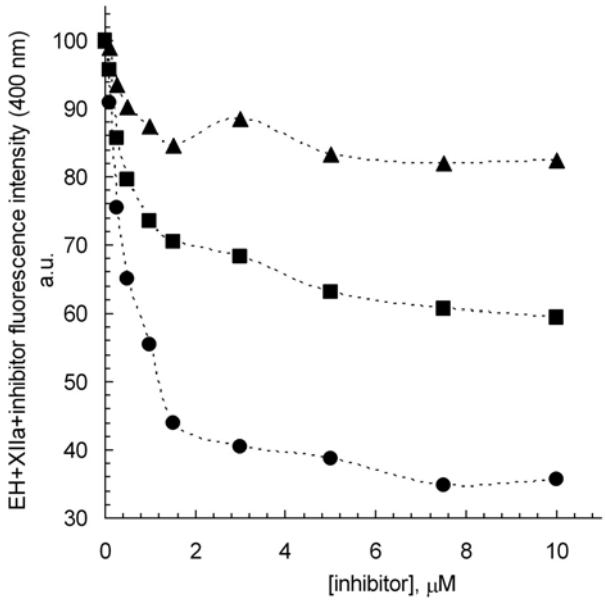

Fig. (8). Quenching of the 392-nm peak (mixture EH + XXa) by other EH inhibitors: effect of the concentration of the other (second) inhibitor on fluorescence intensity of the EH (50 nM) and XXa (2.5 μM) mixture (excited at 290 nm, monitored emission at 400 nm). Second inhibitors: XXV (strong potency, circles); XX (medium potency, squares); and II (low potency, triangles).

CONCLUSIONS

We demonstrated the observation of a strong fluorescent peak at 392 nm when exciting the tryptophans in the mixture of the enzyme EH and its fluorescent inhibitor XIIa. This peak can not be observed in the absence of EH, and is attributed to the inhibitor XIIa bound inside the active center of the EH. We demonstrated a novel fluorescent assay based on the competition of other, otherwise "not visible", strong EH inhibitors, with the XIIa – EH mixture, in order to distinguish these potent EH inhibitors among themselves. This assay does not apply to weak inhibitors but allows to distinguish highly potent inhibitors and to visualize the strongest among them. We generated our assay calibration curve using moderate inhibitors (with IC_{50} higher than 0.05 μM), as well as a low-potency inhibitor with a high IC_{50} value and negligible quenching effect, by plotting quenching strength $K(mix)_{SV}$ versus inhibiting strength, IC_{50} values. Then, we applied this plot to determine IC_{50} values for several highly potent inhibitors, with IC_{50} values at the limit of the IC_{50} detection sensitivity by colorimetric enzyme assay. IC_{50} values determined from our quenching assay show correlation with IC_{50} values determined in the literature by more sensitive radioactive-based assay and allow differentiating the inhibitors' potency in this group. To our knowledge, this is the first inhibitor assay of such kind. This tool may be very important in discovering new inhibitor structures for the therapeutic inhibition of sEH, applied to the treatment of various diseases.

Table 2. Inhibitor Assay: Quenching of the 392-nm-Peak Fluorescence of the Mixture EH+XIIa by Various "Transparent" Strong EH Inhibitors

Inhibitor	Quenching, % (at 2-10 μM of the Transparent Inhibitor)	$K(mix)_{SV}$ (10^6), M^{-1}	mEH IC_{50} (μM) Colorimetric Assay (Measured in this Work)	mEH IC_{50} (μM) Radioactive Assay (from the Literature [27])	mEH IC_{50} (μM) Obtained from the Quenching Assay Data, Fig. (9B)
II	10 ± 5 (10 μM)	0.030	500		
XIX	39 ± 3 (10 μM)	0.189	51.7 ± 0.7		
XX	40 ± 3 (10 μM)	0.326	9.51± 0.09		
XXII	52 ± 2 (10 μM)	0.581	1.7 ± 0.1		
XXIII	46 ± 3 (10 μM)	0.813	0.09 ± 0.01	0.0818±0.0007	
XXIV	52 ± 2 (10 μM)	0.762	0.05 ± 0.01	0.181 ± 0.002	0.16
XXV	66 ± 3 (10 μM)	1.001	0.05 ± 0.01	0.0167 ±0.0005	0.013
XXVI	52 ± 2 (10 μM)	1.045	0.06 ± 0.01	0.0073±0.0001	0.008
XXVII	55 ± 3 (10 μM)	1.06	0.05 ± 0.01		0.007

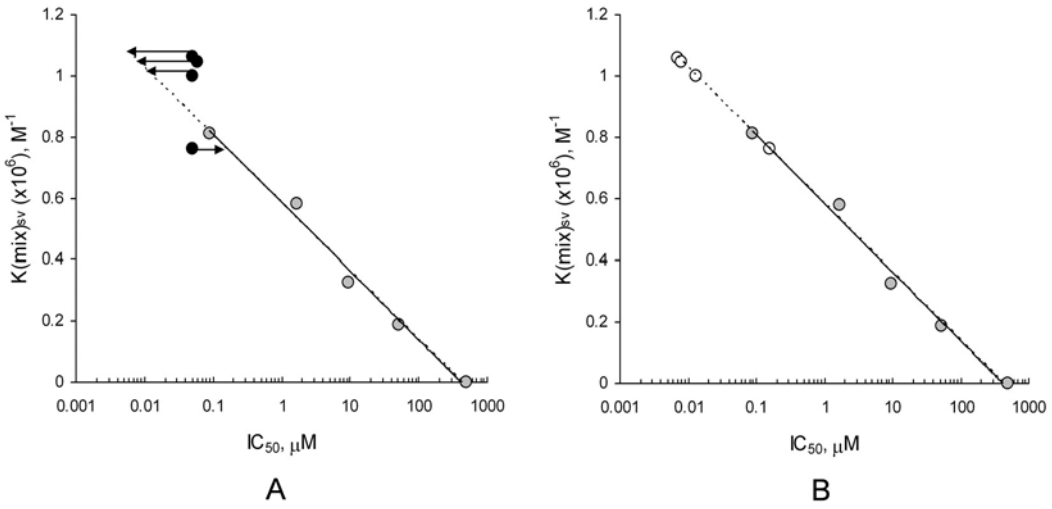

Fig. (9). Quenching assay: correlation between IC_{50} of the 'transparent' inhibitors and their effect on the 392-nm peak from the mixture EH and XXa ([EH] 50 nM, [XXa] 2.5 μM, [transparent inhibitor] 10 μM). Calibration inhibitors: XIX, XX, XXII, XXIII, and II (Table **2**) (grey circles). (**9A**) Black circles: a set of strong inhibitors with IC_{50} values 0.05-0.06 μM, at the limit of the IC_{50} detection sensitivity by colorimetric enzyme assay (Table **1**). Arrows show the application of our calibration plot (grey circles fitting line) to these strong inhibitors and the aligning of all the black circles in the calibration range. (**9B**) White circles: the result of the application of the calibration plot (shown by arrows on Fig. **9A**). IC_{50} values corresponding to the white circles are presented in Table **2**, right column.

ACKNOWLEDGMENTS

This work was supported by Texas Emerging Technologies Fund, NIEHS R37 ES002710, and NIEHS Superfund Basic Research Program, P42 ES004699.

ABBREVIATIONS USED

BCA = Bicinchoninic acid

DBU = 1,8-Diazabicyclo[5.4.0]undec-7-ene

DMF = Dimethylformamide

EH = Epoxide hydrolase

mEH = Microsomal epoxide hydrolase

sEH = Soluble epoxide hydrolase

REFERENCES

[1] Orru, R.V.; Archelas, A.; Furstoss, R. and Faber, K. (1999) Epoxide hydrolases and their synthetic applications. *Adv. Biochem. Eng. Biotechnol*., **63**, 145-167.

[2] Morisseau, C. and Hammock, B.D. (2005) Epoxide hydrolases: mechanisms, inhibitor designs, and biological roles. *Ann. Rev. Pharmacol. Toxicol.,* **45**, 311-333.

[3] Omiecinski, C.J.; Hassett, C. and Hosagrahara, V. (2000) Epoxide hydrolase--polymorphism and role in toxicology. *Toxicol. Lett.,* **112-113**, 365-370.

[4] Newman J.W.; Morisseau, C. and Hammock, B.D. (2005) Epoxide hydrolases: their roles and interactions with lipid metabolism. *Prog. Lipid Res.,* **44**(1), 1-51.

[5] Fang, X.; Hu, S.; Watanabe, T.; Weintraub, N. L.; Snyder, G. D.; Yao, J.; Liu, Y.; Shyy, J.Y.-J.; Hammock, B.D. and Spector, A.A. (2005) Activation of peroxisome proliferator-activated receptor {alpha} by substituted urea-derived soluble epoxide hydrolase inhibitors. *J. Pharmacol. Exp. Ther.,* **314**(1), 260-270.

[6] Chiamvimonvat, N.; Ho, Ch.-M.; Tsai, H.-J. and Hammock, B.D. (2007) The soluble epoxide hydrolase as a pharmaceutical target for hypertension. *J. Cardiovasc. Pharm.,* **50**(3), 225-237.

[7] Inceoglu, B.; Schmelzer, K.R.; Morisseau, C.; Jinks, S.L. and Hammock, B.D. (2007) Soluble epoxide hydrolase inhibition reveals novel biological functions of epoxyeicosatrienoic acids (EETs). *Prostaglandins Other Lipid Mediat.,* **82**(1-4), 42-49.

[8] Seubert, J.M.; Sinal, C.J.; Graves, J.; DeGraff, L.M.; Bradbury, J.A.; Lee, C.R.; Goralski, K.; Carey, M.A.; Luria, A.; Newman, J.W.; Hammock, B.D.; Falck, J.R.; Roberts, H.; Rockman, H.A.; Murphy, E. and Zeldin, D.C. (2006) Role of soluble epoxide hydrolase in postischemic recovery of heart contractile function. *Circ. Res*., **99**(4), 442-450.

[9] Zhang, W.; Koerner, I.P.; Noppens, R.; Grafe, M.; Tsai, H.J.; Morisseau, C.; Luria, A.; Hammock, B.D.; Falck, J.R. and Alkayed, N.J. (2007) Soluble epoxide hydrolase: a novel therapeutic target in stroke. *J. Cereb. Blood Flow Metab*., 1-10.

[10] Hwang, S.H.; Tsai, H.-J.; Liu, J.Y.; Morisseau, C. and Hammock, B.D. (2007) Orally bioavailable potent soluble epoxide hydrolase inhibitors. *J. Med. Chem.* **50**(16), 3825-3840.

[11] Argiriadi, M.A.; Morisseau, C.; Hammock, B.D. and Christianson, D.W. (1999) Detoxification of environmental mutagens and carcinogens: Structure, mechanism, and evolution of liver epoxide hydrolase. *Proc. Nat. Acad. Sci. USA,* **96**(19), 10637-10642.

[12] Argiriadi, M.A.; Morisseau, C.; Goodrow, M.H.; Dowdy, D.L.; Hammock, B.D. and Christianson, D.W. (2000) Binding of alkylurea inhibitors to epoxide hydrolase implicates active site tyrosines in substrate activation. *J. Biol. Chem*., **275**(20), 15265-15270.

[13] Jäger, S.; Brand, L. and Eggeling, C. (2003) New fluorescence techniques for high-throughput drug discovery . *Curr. Pharm. Biotechnol*., **4**(6), 463-476.

[14] Eftink, M.R. and Ghiron, C.A. (1984) Indole fluorescence quenching studies on proteins and model systems: use of the inefficient quencher succinimide. *Biochemistry,* **23**(17), 3891-3899.

[15] Sonveaux, N.; Vigano, C.; Shapiro, A.B.; Ling, V. and Ruysschaert, J.M. (1999) Ligand-mediated tertiary structure changes of reconstituted P-glycoprotein. A tryptophan fluorescence quenching analysis. *J. Biol. Chem*., **274**(25), 17649-17654.

[16] Kleinschmidt, J.H. and Tamm, L.K. (1999) Time-resolved distance determination by tryptophan fluorescence quenching: probing intermediates in membrane protein folding. *Biochemistry,* **38**(16), 4996-5005.

[17] Chadborn, N.; Bryant, J.; Bain, A.J. and O'Shea, P. (1999) Ligand-dependent conformational equilibria of serum albumin revealed by tryptophan fluorescence quenching. *Biophys. J*., **76**(4), 2198-2207.

[18] Kelkar, D.A.; Chattopadhyay, A.; Chakrabarti, A. and Bhattacharyya, M. (2005) Effect of ionic strength on the organization and dynamics of tryptophan residues in erythroid spectrin: a fluorescence approach. *Biopolymers,* **77**(6), 325-334.

[19] Sultan, N.A.; Rao, R.N.; Nadimpalli, S.K. and Swamy, M.J. (2006) Tryptophan environment, secondary structure and thermal unfolding of the galactose-specific seed lectin from Dolichos lablab: fluorescence and circular dichroism spectroscopic studies. *Biochim. Biophys. Acta,* **1760**(7), 1001-1008.

[20] Morisseau, C.; Goodrow, M.H.; Dowdy, D.; Zheng, J.; Greene, J.F.; Sanborn, J.R. and Hammock, B.D. (1999) Potent urea and carbamate inhibitors of soluble epoxide hydrolases. *Proc. Nat. Acad. Sci. USA,* **96**(16), 8849-8854.

[21] Davis, B.B.; Thompson, D.A.; Howard, L.L.; Morisseau, C.; Hammock, B.D. and Weiss, R.H. (2002) Inhibitors of soluble epoxide hydrolase attenuate vascular smooth muscle cell proliferation. *Proc. Natl. Acad. Sci. USA,* **99**(4), 2222-2227.

[22] Kim, I.H.; Morisseau, C.; Watanabe, T. and Hammock, B.D. (2004) Design, synthesis, and biological activity of 1,3-disubstituted ureas as potent inhibitors of the soluble epoxide hydrolase of increased water solubility. *J. Med. Chem*., **47**(8), 2110-2122.

[23] Grant, D.E.; Storms, D.H. and Hammock, B.D. (1993) Molecular cloning and expression of murine liver soluble epoxide hydrolase. *J. Biol. Chem.,* **268**(23), 17628-17633.

[24] Beetham, J.K.; Tian, T. and Hammock, B.D. (1993) cDNA cloning and expression of a soluble epoxide hydrolase from human liver. *Arch. Biochem. Biophys*., **305**(1), 197-201.

[25] Wixtrom, R.N.; Silva, M.H. and Hammock, B.D. (1988) Affinity purification of cytosolic epoxide hydrolase using derivatized epoxy-activated Sepharose gels. *Anal. Biochem*., **169**(1), 71-80.

[26] Dietze, E.C.; Kuwano, E. and Hammock, B.D. (1994) Spectrophotometric substrates for cytosolic epoxide hydrolase. *Anal. Biochem.,* **216**(1), 176-187.

[27] Morisseau, C.; Goodrow, M.H.; Newman, J.W.; Wheelock, C.E.; Dowdy, D.L. and Hammock, B.D. (2002) Structural refinement of inhibitors of urea-based soluble epoxide hydrolases. *Biochem. Pharmacol.,* **63**(9), 1599-1608.

[28] Severson, T.F.; Goodrow, M.H.; Morisseau, C.; Dowdy, D.L. and Hammock, B.D. (2002) Urea and amide-based inhibitors of the juvenile hormone epoxide hydrolase of the tobacco hornworm (Manduca sexta: Sphingidae). *Insect Biochem. Mol. Biol.,* **32**(12), 1741-1756.

[29] McElroy, N.R.; Jurs, P.C.; Morisseau, C. and Hammock, B.D. (2003) QSAR and classification of murine and human soluble epoxide hydrolase inhibition by urea-like compounds. *J. Med. Chem.,* **46**(6), 1066-1080.

[30] Nakagawa, Y.; Wheelock, C.E.; Morisseau, C.; Goodrow, M.H.; Hammock, B.G. and Hammock, B.D. (2000) 3-D QSAR analysis of inhibition of murine soluble epoxide hydrolase (MsEH) by benzoylureas, arylureas, and their analogues. *Bioorg. Med. Chem*., **8**(11), 2663-2673.

[31] Morisseau, C.; Newman, J.W.; Dowdy, D.L.; Goodrow, M.H. and Hammock, B.D. (2001) Inhibition of microsomal epoxide hydrolases by ureas, amides, and amines. *Chem. Res. Toxicol*., **14**(4), 409-415.

[32] Wang, L.; Gaigalas, A.; Abbasi, F.; Marti, G.; Vogt, R. and Schwartz, A. (2002) Quantitating fluorescence intensity from fluorophores: practical use of MESF values. *J. Res. Natl. Inst. Stand. Technol.,* 107, 339-353.

[33] Jones, P.D.; Wolf, N.M.; Morisseau, C.; Whetstone, P.; Hock, B. and Hammock, B.D. (2005) Fluorescent substrates for soluble epoxide hydrolase and application to inhibition studies. *Anal. Biochem*., **343**(1), 66-75.

[34] Borhan, B.; Mebrahtu, T.; Nazarian, S.; Kurth, M.J. and Hammock, B.D. (1995) Improved radiolabeled substrates for soluble epoxide hydrolase. *Anal. Biochem.,* **231**(1), 188-200.

Received: September 09, 2009 **Accepted: November 18, 2009**